Jets, Substructure, and Searching for Dark Matter at the Large Hadron Collider

by

Siddharth Madhavan Narayanan

Submitted to the Department of Physics
in partial fulfillment of the requirements for the degree of

Doctor of Philosophy

at the

MASSACHUSETTS INSTITUTE OF TECHNOLOGY

August 2018

Author .....
Department of Physics
August 32, 2018

Certified by .....
Christoph M. E. Paus
Professor of Physics
Thesis Supervisor

Accepted by .....
Somebody
Chairman, Department Committee on Graduate Theses

Jets, Substructure, and Searching for Dark Matter at the Large Hadron Collider

by

Siddharth Madhavan Narayanan

Submitted to the Department of Physics
on August 32, 2018, in partial fulfillment of the
requirements for the degree of
Doctor of Philosophy

Abstract

Astrophysical observations of gravitational interactions provide strong evidence for the existence of dark matter (DM). Many theories propose and experiments test the hypothesis that DM may have a particle physics origin, but this remains unproven. One such experiment is the Compact Muon Solenoid (CMS) at the Large Hadron Collider (LHC). If DM couples to particles present in protons, it is possible that DM is produced in collisions at the LHC. Because DM is effectively invisible to CMS, we must look for collisions in which DM is produced in association with one or more Standard Model (SM) particles. This thesis describes two different scenarios for the SM particle hypothesis: a single top quark or two light quarks. Both cases result in complicated detector signatures due to the hadronization of final-state quarks. Improved jet substructure techniques to identify some of these unique signatures are presented. Since the observed data is consistent with SM backgrounds in all searches, we translate this result into the most stringent constraints to date on the relevant beyond-SM models.

Thesis Supervisor: Christoph M. E. Paus
Title: Professor of Physics

Contents

Chapter 1

Introduction

1.1 The Standard Model of particle physics

The Standard Model (SM) is a quantum field theory governing the kinematics and interactions of a set of fermion fields, respecting Lorentz and local gauge symmetries. The SM gauge group G decomposes into an electroweak sector (with symmetry group $\mathrm{U}(1)\times\mathrm{SU}(2)$) [1, 2, 3] and a strong sector (SU(3)) [4, 5]. The action of G on a fermion depends on the representation of the Lie group in which the fermion resides and the coupling strength. For the special unitary groups, we denote the representation as $\mathbf{N}$ (fundamental), $\bar{\mathbf{N}}$ (anti-fundamental), or $\mathbf{1}$ (trivial). The special unitary gauges have the same interaction strength for all fermions in non-trivial representations (known as universality). All fermions are in a one-dimensional representation of U(1), but the weak hypercharge (Y_W) distinguishes their transformation under the gauge group $f \mapsto f + iY_W g' f$, where g' is the coupling strength of U(1).

Table 1.1 gives a summary of the *first generation* SM fermion fields and the representation of G which acts on them. The SM provides a total of 3 generations of fermions, each of them copies of the first generation in terms of the field content and gauge group action.

Table 1.1: First generation SM fermions and the action of the SM local gauge symmetry group G. The subscripts L and R refer to left- and right-handed chirality fields. Not shown are the charge conjugated fields $f^C \equiv Cf$, which sit in conjugated representations.

Name	Symbol	Y_W	SU(2) rep.	SU(3) rep.
Left-handed lepton	ℓ_L	$-1/2$	**2**	**1**
Right-handed charged lepton	e_R^-	-1	**1**	**1**
Right-handed neutrino	ν_R	0	**1**	**1**
Left-handed quark	q_L	$1/6$	**2**	**3**
Right-handed up quark	u_R	$2/3$	**1**	**3**
Right-handed down quark	d_R	$-1/3$	**1**	**3**

The lepton doublets contain the left-handed charged leptons and neutral neutrinos:

$$\ell_{iL} = \begin{pmatrix} \nu_e \\ e_L^- \end{pmatrix}, \begin{pmatrix} \nu_\mu \\ \mu_L^- \end{pmatrix}, \begin{pmatrix} \nu_\tau \\ \tau_L^- \end{pmatrix} \tag{1.1}$$

where i indexes the generation. The right handed lepton singlets contain the right-handed projections of the same fermions.

The quark (electroweak) doublets contain the left-handed up- and down-type quarks:

$$q_{iL} = \begin{pmatrix} u_L \\ d'_L \end{pmatrix}, \begin{pmatrix} c_L \\ s'_L \end{pmatrix}, \begin{pmatrix} t_L \\ b'_L \end{pmatrix} \tag{1.2}$$

where d', s', b' represent linear combinations of the mass eigenstates d, s, b (discussed further in Section 1.1.2). All quarks also sit in a strong triplet; we have suppressed its charge above, as the strong representation is orthogonal to the electroweak representation. Where necessary, it will be specified with a superscript, i.e. u^c.

1.1.1 Quantum chromodynamics

The dynamics of quarks under the SU(3) gauge group is commonly referred to as the strong interaction or quantum chromodynamics (QCD). The QCD Lagrangian is:

$$\mathcal{L}_{\text{QCD}} = i\bar{q}_f^a \not{D}^{ab} q_f^b + m_f \bar{q}_f^a q_f^a - \frac{1}{4} G_{\mu\nu}^a G^{a,\mu\nu} \tag{1.3}$$

where repeated indices are contracted; $q_f = u, d, c, s, b, t$ are the spinors for each quark flavor f; $a, b = r, g, b$ are the colors (basis elements of the triplet representation); m_q is the mass of quark flavor q. D_μ is the QCD covariant derivative:

$$D_\mu^{ab} = \delta^{ab}\partial_\mu - ig_s \sum_c t_c^{ab} G_{c,\mu} \tag{1.4}$$

where g_s is the strong coupling strength; t_c are the 8 generators of the triplet representation of SU(3); G_c are the corresponding 8 gauge boson (gluon) fields. $G_{\mu\nu}^a$ are the gluon field strength tensors:

$$G_{\mu\nu}^a = \partial_\mu G_\nu^a - \partial_\nu G_\mu^a - g_s f^{abc} G_\mu^b G_\nu^c \tag{1.5}$$

where f^{abc} are the structure constants of SU(3).

An additional term can be added to Equation 1.3 without violating any guage or Lorentz symmetry or renormalizability. This term would violate CP conservation and produce a non-zero electric dipole moment (EDM) for the neutron. No evidence for such a term has yet been found (although it has not been excluded) [6], and so we do not consider it as part of the SM QCD Lagrangian.

Renormalization and running of couplings

Physical quantities in a QFT (couplings, masses, field strengths, operators) acquire a scale-dependence from higher-order corrections to vertices and propagators. In many cases, the quantum corrections to the bare parameter contain ultraviolet divergent terms. These infinities are absorbed into the Lagrangian by means of adding *counterterms*. The systematic process of absorbing these infinities and ensuring scale-independence is known as renormalization. A Lagrangian is called *renormalizable* if only a finite number of counterterms are needed to ensure that all observables (i.e. amplitudes) are finite. The SM is a renormalizable theory.

In this discussion, we will focus on the renormalization of the coupling $\alpha_S \equiv g_s^2/4\pi$, but the argument applies broadly to all SM quantities. There are two related

consequences of quantum corrections: α_S acquires a non-trivial dependence on the energy scale at which it is probed ($\mu_R^2 = -q^2$, where q^μ is the gluon momentum); and the *bare* α_S as written in the Lagrangian is not the same as the $\alpha_S(\mu_R^2)$ measured in the laboratory. We will refer to the bare coupling as α_{S0}. Note that it does not have a μ_R^2-dependence. To enforce this, we look for solutions to the differential equation

$$\mu_R^2 \frac{\mathrm{d}\alpha_{S0}}{\mathrm{d}\mu_R^2} = 0 \tag{1.6}$$

Writing α_{S0} in terms of α_S (which has a μ_R^2-dependence) and rearranging the terms, we arrive at the β *function* for α_S:

$$\beta(\alpha_S) \equiv \mu_R^2 \frac{\mathrm{d}\alpha_S}{\mathrm{d}\mu_R^2} = -\left(\beta_0 \alpha_S^2 + \beta_1 \alpha_S^3 + \mathcal{O}(\alpha_S^4)\right) \tag{1.7}$$

The β coefficients are:

$$\beta_0 = \frac{33 - 2n_f}{3},\ \beta_1 = \frac{153 - 19n_f}{24\pi^2}, \ldots \tag{1.8}$$

where n_f is the number of quark flavors with masses below μ_R [7, 4, 5]. To one-loop order, the solution to this differential equation is:

$$\alpha_S(\mu_R) = \frac{2\pi}{\beta_0 \ln \frac{\mu_R}{\Lambda_{\mathrm{QCD}}}} \tag{1.9}$$

where Λ_{QCD} is set by enforcing a measured boundary condition, e.g. $\alpha_S(m_Z^2) = 0.1181 \pm 0.0011$ [7]. The exact value of Λ_{QCD} depends on the number of flavors ($n_f = 5$ at m_Z) and the renormalization scheme (most commonly used is $\overline{\mathrm{MS}}$ [8]); with these conditions, $\Lambda_{\mathrm{QCD}} = 218$ MeV. $\beta_0 > 0$ implies α_S falls as a function of energy, as illustrated in Figure 1.1.

This running (the opposite of theories like quantum electrodynamics, in which $\beta_0 < 0$) results in an asymptotically ($\mu_R \to \infty$) free theory. Below Λ_{QCD}, the coupling constant is larger than order unity and perturbative QCD (pQCD) cannot make predictions in this regime. This long-range behavior also means that color triplet

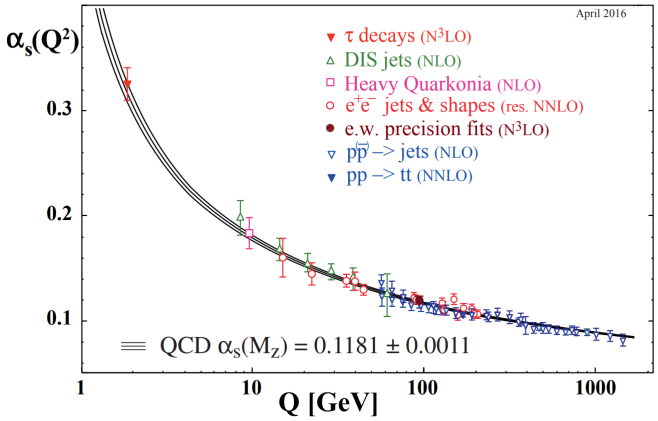

Figure 1.1: Running of the QCD coupling strength α_S as a function of length scale. Reprinted from Reference [7].

.

(quarks, antiquarks) or octet (gluons) states cannot be observed. Only composite singlet states (hadrons) are observable.

1.1.2 Electroweak interactions

The electroweak (EW) sector of the SM refers to the SU(2) × U(1) symmetry group. While all fermion fields in Table 1.1 transform under U(1), only left-handed fermions have non-trivial transformations under SU(2). The EW Lagrangian (ignoring particle masses and the Higgs sector for now) is:

$$\begin{aligned}\mathcal{L}_{\text{EW}} = \; & i\bar{\ell}_{iL}\left(\not{\partial} - ig\not{W}^a\tau^a - ig'Y_{\ell_L}\not{B}\right)\ell_{iL} + i\bar{q}^c_{iL}\left(\not{\partial} - ig\not{W}^a\tau^a - ig'Y_{q_L}\not{B}\right)q^c_{iL} \\ & + i\bar{e}_{iR}\left(\not{\partial} - ig'Y_{e_R}\not{B}\right)e_{iR} + i\bar{u}_{iR^c}\left(\not{\partial} - ig'Y_{u_R}\not{B}\right)u^c_{iR} + i\bar{d}^c_{iR}\left(\not{\partial} - ig'Y_{d_R}\not{B}\right)d^c_{iR} \\ & - \frac{1}{4}W^a_{\mu\nu}W^{a,\mu\nu} - \frac{1}{4}B_{\mu\nu}B^{\mu\nu} \end{aligned} \tag{1.10}$$

where repeated indices are contracted; the subscript i indexes generations; g and g' are respectively the coupling strengths for SU(2) and U(1); Y is the weak hypercharge; W^a_μ are the three gauge fields corresponding to the generators $\tau^a = {}^{\sigma^a}/_2$ of SU(3); B_μ is the gauge field for U(1); and $W^a_{\mu\nu}$ and $B_{\mu\nu}$ are the field strength tensors for the

respective gauge fields. The covariant derivative can be written as:

$$D_\mu = \partial_\mu - ig\delta_L W_\mu^a \tau^a - ig' Y B_\mu \tag{1.11}$$

where Y is the particle's hypercharge and δ_L is 1 if the field is in the **2** representation of SU(2) (e.g. left-handed fermions) and 0 otherwise.

EW symmetry breaking

Unlike Equation 1.3, we cannot introduce a quadratic mass term for fermions in Equation 1.10 because $\bar{\psi}\psi = \psi_R^\dagger \psi_L + \psi_L^\dagger \psi_R$ is not invariant under SU(2) rotations. Spontaneous electroweak symmetry breaking remedies this, as well as provides masses for the gauge fields [9, 10, 11, 12, 13, 14]. A complex scalar doublet ϕ (called the complex Higgs field) with $Y_\phi = 1/2,\ \delta_L = 1$ is added to the Lagrangian:

$$\mathcal{L}_{\text{EW}} \mapsto \mathcal{L}_{\text{EW}} + |D_\mu \phi|^2 + \mu^2 |\phi|^2 - \lambda |\phi|^4 \tag{1.12}$$

We can write the complex doublet as 4 real fields:

$$\phi = \frac{1}{\sqrt{2}} \begin{pmatrix} \phi_1 + i\phi_2 \\ \phi_3 + i\phi_4 \end{pmatrix} \tag{1.13}$$

The two self-interaction terms create a Higgs potential with a degenerate global minimum at *vacuum expectation value* $v \equiv \langle |\phi| \rangle = \sqrt{\mu^2/\lambda}$. Through gauge rotations, we can fix $\langle \phi_{1,2,4} \rangle = 0$ and, at low energies, expand $\phi_3 = v + H$, where H is the real Higgs field. This is the spontaneoous breaking of a symmetry.

By the Nambu-Goldstone theorem [15, 16], these three lost degrees of freedom give rise to three massless bosons. The $|D_\mu \phi|$ term couples the complex Higgs field to the gauge bosons:

$$|D_\mu \phi|^2_{\phi=\langle\phi\rangle} = \frac{v^2}{8} \left[(gW_\mu^1)^2 + (gW_\mu^2)^2 + (g'B_\mu - gW_\mu^3)^2 \right] \tag{1.14}$$

The diagonization of this mass term gives 3 massive weak bosons (consuming the 3

massless Nambu-Goldstone bosons) and one massless photon (defining $\tan\theta_w = g'/g$):

$$\begin{aligned} W_\mu^\pm &\equiv \frac{W_\mu^1 \mp iW_\mu^2}{\sqrt{2}} \\ Z_\mu &\equiv \cos\theta_w W_\mu^3 - \sin\theta_w B_\mu \\ A_\mu &\equiv \sin\theta_w W_\mu^3 + \cos\theta_w B_\mu \end{aligned} \tag{1.15}$$

with mass eigenvalues:

$$m_W = \frac{gv}{2}, \quad m_Z = \frac{v\sqrt{g^2+g'^2}}{2}, \quad m_A = 0 \tag{1.16}$$

The remaining H field, which has not been consumed, is the Higgs boson discovered by CMS and ATLAS [17] in 2012. It has mass $m_H = \sqrt{2}\mu$. By expanding ϕ around $\langle\phi\rangle$ in Equation 1.12, we find couplings to the massive gauge bosons:

$$\begin{aligned} &\frac{m_Z^2}{v} h Z_\mu Z^\mu, \quad \frac{2m_W^2}{v} h W^{+\mu} W_\mu^-, \\ &\frac{m_Z^2}{2v} h^2 Z_\mu Z^\mu, \quad \frac{m_W^2}{v} h^2 W^{+\mu} W_\mu^- \end{aligned} \tag{1.17}$$

The breaking of the SU(2) × U(1) symmetry leaves behind a local U(1) symmetry (with gauge boson A_μ), which corresponds to electromagnetism. Fermions have charge $eQ = e(T_3 + Y)$, where $e = g'\cos\theta_w$ and T_3 is the third isospin component. The $W^\pm$ bosons receive charge $\pm e$. After symmetry breaking, the actions of the broken gauge groups on fermions are governed by the following Lagrangian terms:

$$\begin{aligned} \mathcal{L}_{\text{EWSB}} \supset \sum_f \Bigg[&\bar{f}\left(i\partial\!\!\!/ - eQ_f A\!\!\!/\right) f - \frac{g}{2\sqrt{2}} \bar{f}_L \left(T^+ W\!\!\!/^+ + T^- W\!\!\!/^-\right) f_L \\ &- \frac{g}{2\cos\theta_w} \bar{f}\left(g_{Vf} - g_{Af}\right) Z\!\!\!/ f \Bigg] \end{aligned} \tag{1.18}$$

where f are all fermion fields; $f_L = \frac{1}{2}(1-\gamma^5)f$; $g_V = T_3 - 2Q\sin^2\theta_w$; and $g_A = T_3$.

Fermion masses

The last piece of the EW Lagrangian is the addition of the fermion masses through Yukawa couplings with the Higgs doublet. First, let us add the terms for quark couplings:

$$\mathcal{L}_{\text{EW}} \mapsto \mathcal{L}_{\text{EW}} - y^d_{ij}\bar{q}_{iL}\phi d_{jR} - y^u_{ij}\bar{q}_{iL}i\sigma_2\phi^* u_{uR}i + \text{h.c.} \tag{1.19}$$

where h.c. refers to the Hermetian conjugate of preceding terms; and $y^{u,d}_{ij}$ are the Yukawa matrices for up- and down-type quarks. Breaking the symmetry and collecting terms proportional to v:

$$-\frac{v}{\sqrt{2}}\left(y^d_{ij}\bar{d}'_{iL}d_{jR} + y^u_{ij}\bar{u}_{iL}u_{jR}\right) \tag{1.20}$$

The mass eigenstates are found by diagonalizing these terms, which are written in terms of the weak eigenstates. Let us denote the unitary transformations from the mass basis to the weak basis as U_u and U_d. If we try to write the rest of $\mathcal{L}_{\text{EWSB}}$ in terms of mass eigenstates, we see that terms of the following form all have trivial transformations:

$$\bar{d}'\gamma^\mu d' \mapsto \bar{d}U^\dagger_d\gamma^\mu U_d d = \bar{d}\gamma^\mu d \tag{1.21}$$

The only non-trivial transformation is in the charged weak interaction:

$$\begin{aligned}\bar{u}_L\not{W}^+ d'_L + \bar{d}'_L W^- u_L &\mapsto \bar{u}_L\not{W}^+ U^\dagger_u U_d d_L + \bar{d}_L W^- U^\dagger_d U_u u_L \\ &\equiv \bar{u}_L\not{W}^+ V_{\text{CKM}} d_L + \bar{d}_L W^- V^\dagger_{\text{CKM}} u_L\end{aligned} \tag{1.22}$$

where V_{CKM} is the Cabibbo-Kobayshi-Maskawa matrix [18, 19]. It is nearly-diagonal, but with non-zero mixing between the generations. The CKM matrix also contains a charge parity (CP) violating phase. When referring to down-type quarks, we typically refer to the mass eigenstate d as opposed to d'.

Table 1.2: Summary of the SM fields after electroweak symmery breaking. All masses are taken from the global fits compiled by the Particle Data Group [7].

Name	Symbol	Spin	Mass	Q_e
gluon	g^{ab}	1	0	0
photon	γ	1	0	0
Z boson	Z	1	91.2 GeV	0
W boson	$W^{\pm}$	1	80.4 GeV	± 1
Higgs boson	H	0	125 GeV	0
up quark	u	$1/2$	2.2 MeV	$2/3$
down quark	d	$1/2$	4.7 MeV	$-1/3$
charm quark	c	$1/2$	1.28 GeV	$2/3$
strange quark	s	$1/2$	95 MeV	$-1/3$
top quark	t	$1/2$	173 GeV	$2/3$
bottom quark	b	$1/2$	4.18 GeV	$-1/3$
electron neutrino	ν_e	$1/2$	–	0
electron	e	$1/2$	511 keV	-1
muon neutrino	ν_μ	$1/2$	–	0
muon	μ	$1/2$	105 MeV	-1
tau neutrino	ν_τ	$1/2$	–	0
tau	τ	$1/2$	178 GeV	-1

A similar analysis can be carried out for the lepton sector:

$$\mathcal{L}_{\text{EW}} \mapsto \mathcal{L}_{\text{EW}} - y^e_{ij}\bar{\ell}_{iL}\phi e_{jR} - y^\nu_{ij}\bar{\ell}_{iL}i\sigma_2\phi^*\nu_{uR}i + \text{h.c.} \tag{1.23}$$

The mixing matrix for leptons is the Pontecorvo-Maki-Nakagawa-Sakata matrix U_{PMNS} [20], which relates the weak eigenstates ν_e, ν_μ, ν_τ with the mass eigenstates ν_1, ν_2, ν_3. The values of the neutrino masses are known to be non-zero from the observation of neutrino oscillations [21].

After EWSB, each fermion mass eigenstate has a mass term and coupling to the Higgs field:

$$\mathcal{L}_{\text{EWSB}} \supset \sum_f -\frac{y_f v}{\sqrt{2}}\left(\bar{f}f + \bar{f}Hf\right) \tag{1.24}$$

where we identify the mass as $m_f = y_f v/\sqrt{2}$. Table 1.2 summarizes all SM fermions and some of their properties after EWSB.

1.2 Dark matter

While the SM is incredibly powerful at predicting the outcomes of many laboratory experiments, there are certain major phenomena it cannot predict:

- There is not yet a complete formulation of *quantum gravity*, folding in general relativity [22].
- The observed *matter/antimatter asymmetry* in the universe cannot be explained by the SM's CP violation and (predicted) baryon number of violation. Additional CP and B violating interactions must exist.
- *Neutrino masses* are not completely determined by the SM. While a mass term can be written down as in Section 1.1.2, it does not exclude a Majorana mass term for right-handed neutrinos. Nor does it explain the observed range of masses $m_\nu/m_t \lesssim 10^{-15}$.
- An explanation of *dark energy* accounting for $\Omega_\Lambda h \sim 68\%$ of the universe's energy budget, suggested by measurements of the CMB, galaxy clusters, supernovae, and other measurements of the universe expansion rate [23].
- An explanation of *dark matter* accounting for $\Omega_{\rm DM} h \sim 20\%$ of the universe's energy budget, suggested by measurements of galactic rotation curves, the CMB, and gravitational lensing [7, 24, 25, 26].

In this thesis, we describe tests of certain extensions of the SM which add candidate fields for dark matter (DM).

Astrophysical evidence

All known evidence of DM arises from gravitational measurements. One of the oldest observations is that of galactic rotational curves. The rotational velocities of stars and hydrogen clouds are measured in galaxies, as a function of distance from the center of the galaxy. It is found that the velocity increases as a function of r, eventually reaching a plateau that extends well past the bulk of the visible mass of the galaxy.

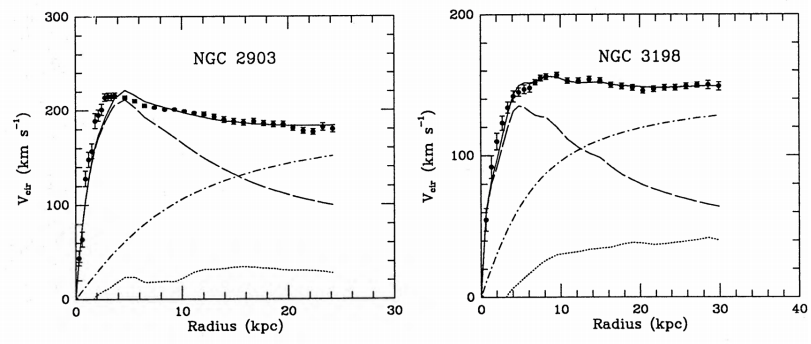

Figure 1.2: Observed and fitted galactic rotational curves for two galaxies. The total fit (solid line) has three components: visible (dashed), gas clouds (dotted), and DM (dash-dotted). Reprinted from Reference [27].

This implies the existence of a massive dark halo that encompasses the galaxy. Indeed, the observed rotational curves $v(r)$ are well-described by a 3 component fit: the visible disk, a gas cloud, and a dark halo. Two galaxies are shown in Figure 1.2, and it is clear that a non-zero DM component is needed to describe the data.

An orthogonal piece of evidence comes from measuring anisotropies in the cosmic microwave background (CMB). The CMB is the remnant of photons after they decoupled from matter in the early universe. The temperature spectrum of the CMB is isotropic to one part in 10^5, and the anisotropies are driven by matter anisotropies at the time of decoupling. The power spectrum of the temperature anisotropies is modified when there are two matter populations (SM and DM) as opposed to one (just SM), especially when the two populations interact with each other (via gravity) but one does not interact with photons (DM). Figure 1.3 shows the power spectrum measured by the Planck experiment [28], compared to the best-fit Λ Cold Dark Matter (ΛCDM) model.

1.3 LHC phenomenology

The Large Hadron Collider collides protons at a center of mass energy $\sqrt{s} = 13$ TeV. Section **??** provides an overview of the LHC machine. In this section, we describe the methods used to make predictions of observables at the LHC. These observables

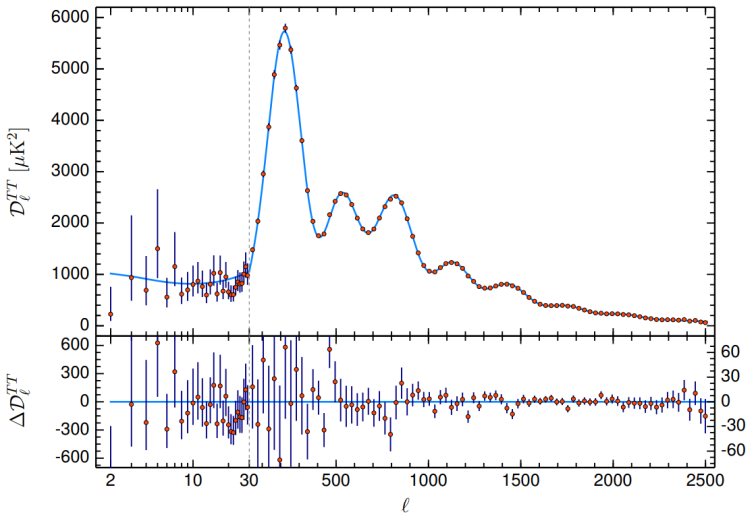

Figure 1.3: Temperature anisotropy power spectrum of the CMB, as measured by Planck. Reprinted from Reference [28].

typically take the form of differential cross sections $\mathrm{d}\sigma(pp \to X)/\mathrm{d}\Theta$, where X is some interesting final state with N particles and Θ is a set of interesting kinematics. The differential element of the general cross section for $2 \to N$ processes is:

$$\mathrm{d}\sigma(ab \to \{c_i\}) = \frac{1}{2s}\left(\prod_i \frac{\mathrm{d}^3 p_i}{(2\pi)^3}\frac{1}{2E_i}\right) \cdot (2\pi)^4 \delta^4\left(k_a + k_b - \sum_i p_i\right) \cdot |\mathcal{M}(ab \to \{c_i\})|^2 \tag{1.25}$$

where k_a, k_b are the incoming momenta; $\{p_i\}$ are the outgoing momenta; and $\mathcal{M}$ is the matrix element of this reaction.

Hadron collisions do not have two-particle initial states, but rather two composite particles containing partons with varying momenta. The general cross section for $pp \to X$ is [29]:

$$\mathrm{d}\sigma(pp \to X(\Theta)) = \sum_{a,b} \int \mathrm{d}x_a \mathrm{d}x_b \, f_a(x_a, \mu_F) f_b(x_b, \mu_F) \cdot \mathrm{d}\sigma(ab \to \{c_i\}) \cdot D(\{c_i\} \to X(\Theta)) \tag{1.26}$$

The sum over a, b refers to summing over partons in the initial state. The momentum fractions of the partons, $x_{a,b}$, follow parton distribution functions (PDFs) $f_{a,b}$ that depend on the particle species a and b. We then define an intermediate state $\{c_i\}$

which evolves into the final state $X(\Theta)$. That is, the process $ab \to X$ is split into $ab \to \{c_i\} \to X$. The definition of $\{c_i\}$ is not unique, but is chosen such that the process $ab \to \{c_i\}$ can be analyzed perturbatively. The non-perturbative aspects of evolution to the final state (soft or collinear radiation) will be analyzed separately. The matrix element for the first step (*hard scattering*) is computed perturbatively and turned into a cross section by means of Equation 1.26. Other heuristic methods are used to deal with the second step (*parton shower* (PS)), encoded in the *fragmentation function* D.

The ability to partition the calculation into perturbative (hard scattering) and non-perturbative (PDF and parton shower) components follows from the collinear factorization theorem [30]. The factorization depends on an arbitrary energy scale μ_F, which defines a lower bound for interactions considered part of the hard scattering. The remainder of this section discusses the use of Monte Carlo (MC) methods to simulate these three factors: f, $\mathcal{M}$, and D.

1.3.1 Parton distribution functions

The analytic behavior of PDFs as a function of the factorization scale is governed by the DGLAP evolution equation [31, 32, 33]:

$$\mu_F \frac{\mathrm{d}}{\mathrm{d}\mu_F} f_a(x_a, \mu_F) = \frac{\alpha_S}{\pi} \int_x^1 \frac{\mathrm{d}y}{y} f_a(y, \mu_F) P_{qq}\left(\frac{x}{y}\right) \tag{1.27}$$
$$\text{where } P_{qq}(z) = \frac{4}{3}\left[\frac{1+z^2}{1-z}\right]_+ + 2\delta(1-z)$$

The computation of f_a for a fixed scale cannot be done analytically. Instead, data from many experiments are used to fit a parameterization, as is done by the NNPDF collaboration [34]. Results presented in this thesis use the NNPDF3.0 PDF set.

1.3.2 Hard scattering

Monte Carlo generators simulate Equation 1.25 by sampling events with probability proportional to the phase space and matrix element. The dedicated MC generators

Table 1.3: Summary of MC generators used for each SM and signal process. Note that the V+jet processes have two entries each in this table, at different QCD orders. Both will be used to improve the prediction accuracy.

$pp \to X$	Generator	NLO in QCD?	Notes
$t\bar{t}$	Powheg	✓	
t, tW, tZ	Powheg	✓	
ZZ, WZ, WW	Pythia		
Z (+0,1 partons)	MG	✓	
W (+0,1 partons)	MG	✓	
γ (+0,1 partons)	MG	✓	
Z (+0,1,2,3 partons)	MG		
W (+0,1,2,3 partons)	MG		
γ (+0,1,2 partons)	MG		
Multijet	MG		Jets defined in Section 1.3.3
Resonant DM	MG		See Chapter **??**
FCNC DM	MG	✓	See Chapter **??**
VBF $H \to \chi\bar{\chi}$	Powheg		See Chapter **??**

used in this result are MadGraph5 [35, 36] and Powheg2 [37]. Both generators can simulate to leading order (LO) in EW vertices and up to next-to-leading order (NLO) in QCD vertices. Finally, the PS model Pythia8.2 [38] (discussed in the next section) can also generate certain hard scattering processes at LO in QCD.

MC generators also generate additional partons from initial and final state radiation as part of the hard scattering. These quarks, gluons, and photons can be highly energetic in events with large q^2, and so it is necessary to compute them as part of the hard scattering matrix element. It should be noted that, while NLO event generation is always preferable, it comes with two costs: (a) being able to generate fewer additional partons and (b) additional computational time. We will use LO simulation for processes which have large cross sections and in which additional parton spectra are important. Table 1.3 provides a summary of the MC generators and orders used in these results.

1.3.3 Parton shower

Suppose we know $\mathrm{d}\sigma(ab \to \{c_i\})$ and would like to know $\mathrm{d}\sigma(ab \to \{c_i\}j)$, where j is radiated from one of the c_i in the soft and/or collinear limit. Such "splittings" include:

$$q \to qg, \quad g \to qq, \quad g \to gg,$$
$$f \to f\gamma, \quad \gamma \to ff \tag{1.28}$$

Define z to be the fraction of energy kept by the parent parton and θ to be the opening angle between c_i and j. For QCD splittings, the cross section can be written (at LO):

$$\mathrm{d}\sigma(ab \to \{c_i\}j) = P_{c_i \to c_i j}(z) \cdot \frac{\alpha_S}{2\pi} \cdot \frac{\mathrm{d}\theta}{\theta}\, \mathrm{d}z\, \mathrm{d}\sigma(ab \to \{c_i\}) \tag{1.29}$$

where $P_{c_i \to c_i j}$ are *splitting functions* analogous to the ones that arise in the DGLAP evolution (Equation 1.3.1). As an example, the splitting function for $q \to qg$ is [38]:

$$P_{q \to qg} = \frac{4}{3}\frac{1+z^2}{1-z} \tag{1.30}$$

It should be noted that this cross section grows as $\theta \to 0$ and $z \to 1$, i.e. soft and collinear splittings. That is, if a bare quark is produced in an event, it will produce many soft and collinear gluons (which in turn can split to qq and gg) prior to hadronization. This iterative process is known as the *parton shower*. As the width of the parton shower nears $1/\Lambda_{\mathrm{QCD}}$, the partons will hadronize, preventing further splitting. These hadronic endpoints of the shower reach the detector and appear as collimated sprays of hadrons (*jets*). The reconstruction of jets is described in detail in Section **??** and Chapter **??**.

PS models simulate the shower and hadronization processes. The results in this thesis use Pythia8.2 [38] which employs the Lund string model [39] to simulate hadronization.

Bibliography

[1] S. Weinberg, "A Model of Leptons," *Phys. Rev. Lett.*, vol. 19, pp. 1264–1266, 1967.

[2] A. Salam, "Weak and Electromagnetic Interactions," *Conf. Proc.*, vol. C680519, pp. 367–377, 1968.

[3] S. L. Glashow, "Partial Symmetries of Weak Interactions," *Nucl. Phys.*, vol. 22, pp. 579–588, 1961.

[4] D. J. Gross and F. Wilczek, "Ultraviolet Behavior of Nonabelian Gauge Theories," *Phys. Rev. Lett.*, vol. 30, pp. 1343–1346, 1973. [,271(1973)].

[5] H. D. Politzer, "Reliable Perturbative Results for Strong Interactions?," *Phys. Rev. Lett.*, vol. 30, pp. 1346–1349, 1973. [,274(1973)].

[6] B. Graner, Y. Chen, E. G. Lindahl, and B. R. Heckel, "Reduced Limit on the Permanent Electric Dipole Moment of Hg^{199};," *Phys. Rev. Lett.*, vol. 116, p. 161601, Apr. 2016.

[7] "Review of particle physics," *Phys. Rev. D*, vol. 98, p. 030001, Aug 2018.

[8] S. Weinberg, "New approach to the renormalization group," *Phys. Rev.*, vol. D8, pp. 3497–3509, 1973.

[9] F. Englert and R. Brout, "Broken Symmetry and the Mass of Gauge Vector Mesons," *Phys. Rev. Lett.*, vol. 13, pp. 321–323, 1964. [,157(1964)].

[10] P. W. Higgs, "Broken symmetries, massless particles and gauge fields," *Phys. Lett.*, vol. 12, pp. 132–133, 1964.

[11] P. W. Higgs, "Broken Symmetries and the Masses of Gauge Bosons," *Phys. Rev. Lett.*, vol. 13, pp. 508–509, 1964. [,160(1964)].

[12] P. W. Higgs, "Spontaneous Symmetry Breakdown without Massless Bosons," *Phys. Rev.*, vol. 145, pp. 1156–1163, 1966.

[13] G. S. Guralnik, C. R. Hagen, and T. W. B. Kibble, "Global Conservation Laws and Massless Particles," *Phys. Rev. Lett.*, vol. 13, pp. 585–587, 1964. [,162(1964)].

[14] T. W. B. Kibble, "Symmetry breaking in nonAbelian gauge theories," *Phys. Rev.*, vol. 155, pp. 1554–1561, 1967. [,165(1967)].

[15] Y. Nambu, "Quasi-Particles and Gauge Invariance in the Theory of Superconductivity," *Physical Review*, vol. 117, pp. 648–663, Feb. 1960.

[16] J. Goldstone, "Field theories with Superconductor solutions," *Il Nuovo Cimento*, vol. 19, pp. 154–164, Jan. 1961.

[17] G. Aad *et al.*, "Combined Measurement of the Higgs Boson Mass in *pp* Collisions at $\sqrt{s} = 7$ and 8 TeV with the ATLAS and CMS Experiments," *Phys. Rev. Lett.*, vol. 114, p. 191803, 2015.

[18] N. Cabibbo, "Unitary Symmetry and Leptonic Decays," *Physical Review Letters*, vol. 10, pp. 531–533, June 1963.

[19] M. Kobayashi and T. Maskawa, "CP-Violation in the Renormalizable Theory of Weak Interaction," *Progress of Theoretical Physics*, vol. 49, pp. 652–657, Feb. 1973.

[20] Z. Maki, M. Nakagawa, and S. Sakata, "Remarks on the Unified Model of Elementary Particles," *Progress of Theoretical Physics*, vol. 28, pp. 870–880, Nov. 1962.

[21] Y. Fukuda *et al.*, "Evidence for Oscillation of Atmospheric Neutrinos," *Physical Review Letters*, vol. 81, pp. 1562–1567, Aug. 1998.

[22] A. Einstein, "Die Feldgleichungen der Gravitation. (German) [The field equations of gravitation]," *Ständiger Beobachter der Preussischen Akademie der Wissenschaften, Part 2*, pp. 844–847, 1915.

[23] P. J. E. Peebles and B. Ratra, "The Cosmological constant and dark energy," *Rev. Mod. Phys.*, vol. 75, pp. 559–606, 2003. [,592(2002)].

[24] G. Bertone, D. Hooper, and J. Silk, "Particle dark matter: evidence, candidates and constraints," *Physics Reports*, vol. 405, p. 279, 2005.

[25] J. L. Feng, "Dark matter candidates from particle physics and methods of detection," *Ann. Rev. Astron. Astrophys.*, vol. 48, p. 495, 2010.

[26] T. A. Porter, R. P. Johnson, and P. W. Graham, "Dark matter searches with astroparticle data," *Ann. Rev. Astron. Astrophys.*, vol. 49, p. 15, 2011.

[27] K. G. Begeman, A. H. Broeils, and R. H. Sanders, "Extended rotation curves of spiral galaxies - Dark haloes and modified dynamics," *Monthly Notices of the Royal Astronomical Society*, vol. 249, pp. 523–537, Apr. 1991.

[28] N. Aghanim *et al.*, "Planck 2018 results. VI. Cosmological parameters," 2018.

[29] M. Perelstein, "Introduction to Collider Physics," pp. 421–486, 2011.

[30] J. C. Collins, D. E. Soper, and G. F. Sterman, "Factorization of Hard Processes in QCD," *Adv. Ser. Direct. High Energy Phys.*, vol. 5, pp. 1–91, 1989.

[31] Y. L. Dokshitzer, "Calculation of the Structure Functions for Deep Inelastic Scattering and e+ e- Annihilation by Perturbation Theory in Quantum Chromodynamics.," *Sov. Phys. JETP*, vol. 46, pp. 641–653, 1977. [Zh. Eksp. Teor. Fiz.73,1216(1977)].

[32] G. Altarelli and G. Parisi, "Asymptotic Freedom in Parton Language," *Nucl. Phys.*, vol. B126, pp. 298–318, 1977.

[33] V. N. Gribov and L. N. Lipatov, "Deep inelastic e p scattering in perturbation theory," *Sov. J. Nucl. Phys.*, vol. 15, pp. 438–450, 1972. [Yad. Fiz.15,781(1972)].

[34] R. D. Ball *et al.*, "Parton distributions for the LHC Run II," *JHEP*, vol. 04, p. 040, 2015.

[35] J. Alwall, R. Frederix, S. Frixione, V. Hirschi, F. Maltoni, O. Mattelaer, H. S. Shao, T. Stelzer, P. Torrielli, and M. Zaro, "The automated computation of tree-level and next-to-leading order differential cross sections, and their matching to parton shower simulations," *JHEP*, vol. 07, p. 079, 2014.

[36] R. Frederix and S. Frixione, "Merging meets matching in MC@NLO," *JHEP*, vol. 12, p. 061, 2012.

[37] C. Oleari, "The POWHEG BOX," *Nuclear Physics B Proceedings Supplements*, vol. 205, pp. 36–41, Aug. 2010.

[38] T. SjÃűstrand, S. Ask, J. R. Christiansen, R. Corke, N. Desai, P. Ilten, S. Mrenna, S. Prestel, C. O. Rasmussen, and P. Z. Skands, "An Introduction to PYTHIA 8.2," *Comput. Phys. Commun.*, vol. 191, pp. 159–177, 2015.

[39] B. Andersson, G. Gustafson, G. Ingelman, and T. Sjostrand, "Parton Fragmentation and String Dynamics," *Phys. Rept.*, vol. 97, pp. 31–145, 1983.